DRAFT VERSION 2023-08-08
Typeset using LaTeX **twocolumn** style in AASTeX63

Snowflakes in a furnace: formation of CO and dust in a recurrent nova eruption

D. P. K. BANERJEE [1], C. E. WOODWARD [2], V. JOSHI [1], A. EVANS [3], F. M. WALTER [4], G. H. MARION [5], E. Y. HSIAO [6], N. M. ASHOK [1], R. D. GEHRZ [2] AND S. STARRFIELD [7]

[1] *Physical Research Laboratory, Navrangpura, Ahmedabad, Gujarat 380009, India*
[2] *Minnesota Institute for Astrophysics, University of Minnesota, 116 Church Street SE, Minneapolis, MN 55455, USA*
[3] *Astrophysics Group, Keele University, Keele, Staffordshire, ST5 5BG, UK*
[4] *Department of Physics and Astronomy, Stony Brook University, Stony Brook, NY 11794-3800*
[5] *Department of Astronomy, University of Texas at Austin, 515 Speedway, Stop C1400, Austin, Texas 78712-1205, USA*
[6] *Department of Physics, Florida State University, 77 Chieftan Way, Tallahassee, FL 32306, USA*
[7] *School of Earth & Space Exploration, Arizona State University, Box 871404, Tempe, AZ 85287-1404, USA*

(Received 2023-06-28; Revised 2023-08-1; Accepted 2023-08-04; Published To appear in the ApJL)

ABSTRACT

We report the detection of carbon monoxide (CO) and dust, formed under hostile conditions, in recurrent nova V745 Sco about 8.7 days after its 2014 outburst. The formation of molecules or dust has not been recorded previously in the ejecta of a recurrent nova. The mass and temperature of the CO and dust are estimated to be $T_{CO} = 2250 \pm 250$ K, $M_{CO} = (1 - 5) \times 10^{-8}\ M_\odot$ and $T_{dust} = 1000 \pm 50$ K , $M_{dust} \sim 10^{-8} - 10^{-9}\ M_\odot$ respectively. At the time of their detection, the shocked gas was at a high temperature of $\sim 10^7$ K as evidenced by the presence of coronal lines. The ejecta were simultaneously irradiated by a large flux of soft X-ray radiation from the central white dwarf. Molecules and dust are not expected to form and survive in such harsh conditions; they are like snowflakes in a furnace. However, it has been posited in other studies that, as the nova ejecta plow through the red giant's wind, a region exists between the forward and reverse shocks that is cool, dense and clumpy where the dust and CO could likely form. We speculate that this site may also be a region of particle acceleration, thereby contributing to the generation of γ-rays.

Keywords: Recurrent novae (1336), Chemical abundances (224), Dust shells (414), Explosive Nucleosynthesis (503)

1. INTRODUCTION

A classical nova eruption results from a thermonuclear runaway (TNR) on the surface of a white dwarf (WD) accreting material from a companion star in a close binary system. The accreted hydrogen-rich material forms a degenerate layer on the WD's surface with the mass of the layer gradually increasing with time. As the accreted matter is compressed and heated by the gravity of the WD, the critical temperature and pressure at the base of the layer reach the ignition point for the TNR that produces the nova eruption. Observationally, the outburst is accompanied by ejection of $\simeq 10^{-6} - 10^{-4}\ M_\odot$ of matter at high velocities and a large brightening, generally with an amplitude of 7 to 15 mags. In time mass-transfer from the secondary resumes, leading to another eruption. All novae recur, but some do so on human ($\lesssim 100$ yrs) timescales. To distinguish them from "classical novae" (CNe), which have inter-eruption periods of $\simeq 10^4$ yrs, these are the "recurrent novae" (RNe), defined by the selection effect that they have been seen to undergo more than one explosion.

Currently there are 10 known Galactic RNe (T Pyx, IM Nor, CI Aql, V2487 Oph, U Sco, V394 CrA, V745 Sco, T CrB, RS Oph, and V3890 Sgr) of which the last four belong to a sub-class having red giant (RG) secondaries. The secondary in V745 Sco has been classified as a giant implied by the luminosity class III M6$\pm$2 (Duerbeck 1989; Sekiguchi et al. 1990; Williams et al. 1991; Harrison et al. 1993; Anupama & Mikołajewska 1999) with an orbital period of 2440 $\pm$ 500 days (Schaefer 2022a). V745 Sco is a very fast nova with t_2 and t_3 of 6.2 and 9 days respectively (t_2, [t_3] is the elapsed time to decline 2 [3] mags from peak brightness).

Corresponding author: C.E. Woodward
mailto:chickw024@gmail.com

V745 Sco lies at a distance of $\simeq 8 \pm 1$ kpc in the Galactic bulge (Schaefer 2022a).

Because the RG secondary in V745 Sco (and in RS Oph-type systems in general) is expected to have a substantial wind, the high-velocity ejecta from the nova eruption plows into the RG wind creating a strong shock resulting in γ-ray and X-ray emission (Cheung et al. 2014; Drake et al. 2016; Orio et al. 2015; Page et al. 2015), optical and near-infrared coronal line emission (Duerbeck 1989, this paper) and non-thermal radio emission (Kantharia et al. 2015). The shocked gas has high temperatures, $10^7 - 10^8$ K (Banerjee et al. 2014; Orio et al. 2015; Drake et al. 2016), producing hard X-rays and coronal lines associated with highly-ionized atoms (e.g., [Fe XIV], IP = 361 eV).

Further, the ejecta are subjected to additional x-ray radiation from the central ionizing source during the supersoft phase recorded between days 3 to 10 (Page et al. 2015; Drake et al. 2016). This is the earliest onset of the SSS phase in a nova. In such a harsh environment, molecules and dust cannot form or survive. Yet, the main result of this work shows that carbon monoxide (CO) and dust *did form* in V745 Sco between 8 to 10 days after outburst.

The formation of either dust or CO in the ejecta proper of a RNe is unprecedented though dust features have been detected in the winds of the RG components of both RS Oph (Evans et al. 2007) and V745 Sco itself (Evans et al., in preparation). In both cases the features arise in dust that is a permanent feature of the binary. Here, we estimate the mass and temperature of the CO and dust and also investigate the formation site.

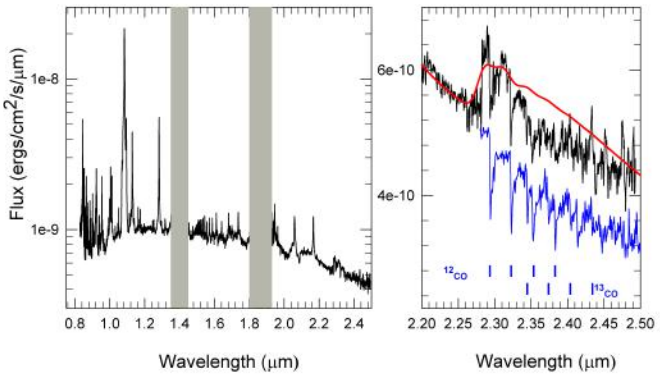

Figure 1. The left panel shows the entire NIR spectrum (available as data behind the figure) of V745 Sco 8.7d after the 2014 eruption (Banerjee et al. 2014). The right panel shows a magnified view of the first overtone CO emission (black). Superposed on the emission are the absorption band heads of ^{12}CO and ^{13}CO (vertical ticks). The spectrum of a typical M6 III, HD 18191 (blue), is also included to show the expected CO absorption band heads. The red line is an LTE model fit to the CO emission. The flux axes in both panels have the same units.

2. RESULTS

2.1. *Carbon monoxide in emission*

Figure 1 shows the near infrared (NIR) spectrum ($R \simeq 6000$, λ = 0.8 - 2.5 μm) of V745 Sco on 2014 Feb 15.46 (+8.7 d after outburst) obtained using the Folded Port Infrared Echellette (FIRE, Simcoe et al. 2008) spectrograph on the 6.5m Magellan Baade Telescope. These data, presented by Banerjee et al. (2014) and which were focused on the shock evolution, are re-examined here. Figure 1 right panel, shows a magnified view of the first overtone CO in emission. Superposed on the emission are ^{12}CO and ^{13}CO bandheads (marked in blue) which most likely arise from the secondary with perhaps some contribution from neutral portions of the equatorial density enhancement discussed later in section 2.3. Absorption bands are expected from the cool secondaries in RS Oph-type systems – it is the emission feature that is so unexpected. CO in emission is not seen that often in novae. When it is detected it is always in FeII-type novae (Banerjee et al. 2016), generally forming at maximum light (e.g., V705 Cas; Evans et al. 1996) or a few weeks thereafter and being subsequently rapidly destroyed in a few days to weeks. It invariably precedes dust formation in CNe. Its duration and the rapidity of its destruction are not understood (Pontefract & Rawlings 2004), but are clearly seen V2615 Oph (Das et al. 2009) and V3662 Oph (Joshi et al. 2017). Banerjee et al. (2016) provide a list of CO forming novae and their CO emission properties up until 2015. Since 2015, four additional novae (V6567 Sgr, V435 CMa, V3662 Oph, V1391 Cas) have CO detections (Joshi et al. 2017; Rudy et al. 2018; Russell et al. 2020; Woodward et al. 2020).

We have estimated the mass of CO using the LTE model developed by Das et al. (2009), which assumes optically thin emission. Adopting d = 8 kpc, the temperature and mass are found to be 2250 $\pm$ 250K, $M_{CO} = (1 - 5) \times 10^{-8}\ M_\odot$. These are typical of values found in other novae and shows that in V745 Sco a substantial amount of CO was formed. For any other choice of distance, the CO mass scales as $(d/8\ \mathrm{kpc})^2$. The FWHM of each ro-vibrational line is found to be 2600 $\pm$ 300 km s^{-1} (close to the 2200 km s^{-1} FWHM of the Paβ line in Banerjee et al. 2014). This indicates a high expansion velocity and explains the lack of band heads in the emission feature. It also implies that the emission originates from high velocity material i.e., from material associated with the shocked gas. It cannot originate from the distant unshocked RG wind which would typically have a small expansion velocity of 5 to 10 km s^{-1}. The CO emission is also seen to be blueshifted by $\simeq$ 2000 km s^{-1}, the reason for which is discussed in section 2.3.

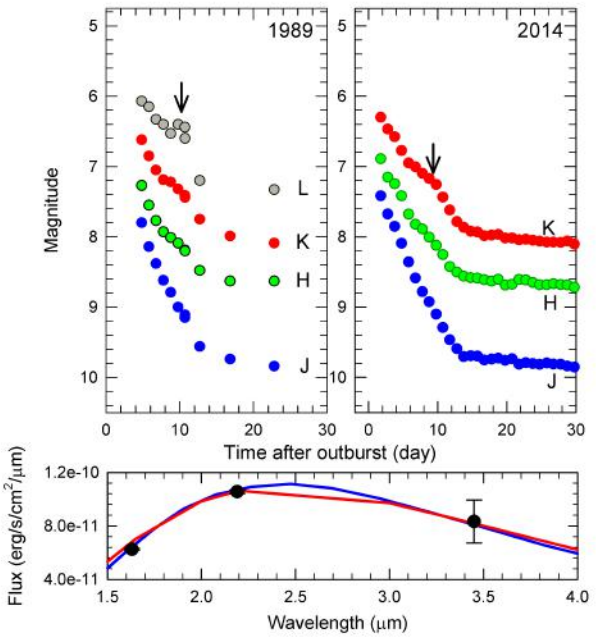

Figure 2. The top two panels show the JHK(L) light curves from the 1989 (Sekiguchi et al. 1990) and the 2014 eruption (ANDICAM data). The error bars in the plots are smaller than the symbol sizes. An IR excess due to dust is seen around day 9. The bottom panel shows the SED of the excess fitted with model fits of silicate (red) and amorphous carbon (blue) dust.

2.2. *Dust in the ejecta*

Dust too appears to have formed in the ejecta around the time that CO was detected. Figure 2, upper right panel, shows high cadence JHK photometry from the Cerro Tololo 1.3-m (+ANDICAM, Walter et al. 2012). Between days 8 to 11, a clear bump is seen in the K band (marked by the arrow) and also in the H band albeit to a lesser extent. The bump is also present in the JHKL photometry of the 1989 eruption (Sekiguchi et al. 1990) which is shown in the upper left panel. Again, the IR excess is seen in the H and K bands and most prominently in the L band. We interpret this IR excess as emission by dust. This interpretation is consistent with the simultaneous appearance of CO. As mentioned earlier, all novae that have shown CO in emission have invariably proceeded to form dust. From the NIR light curves, the maximum excess over the local continuum, assumed linear in the region between 7 to 12 days, is measured to be δH = 0.062 $\pm$ 0.010 and δK = 0.155 $\pm$ 0.014 for the ANDICAM data and δL = 0.360 $\pm$ 0.2 for the Sekiguchi et al. (1990) L band data. Converting these into fluxes, after dereddening using E_{B-V}= 1.0 (Schaefer 2022a,b), and assuming that the L band excess would be the same in both 1989 and 2014, the spectral energy distribution (SED) of the excess based on the HKL fluxes is shown in the bottom panel of Figure 2.

There is good evidence for dust with the SED being well fit by models (based on the formalism of Banerjee et al. 2023, in press) comprising of silicate (Draine & Lee 1984) or amorphous carbon (ACAR sample, Zubko et al. 1996) dust grains. Assuming the dust emission is optically thin and d = 8 $\pm$ 1 kpc, a dust mass and dust temperature of 10^{-8} – 10^{-9} $M_{\odot}$ and 1000 ± 50 K respectively are suggested for both silicates and amorphous carbon grains. The dust mass is within the range typically observed in novae (Gehrz et al. 1998; Evans & Gehrz 2022). Lastly, even if the L datum is excluded from the fit in the bottom panel because it is not contemporaneous with the H and K data, the H and K points taken by themselves show a rising continuum indicating dust

The dust temperature is considerably lower than the condensation temperature of $\sim$ 2000 K for carbon dust, and closer to the condensation temperatures of silicates like forsterite, 1440 K and enstatite, 1350 K (Speck et al. 2000). The most likely condensate is therefore silicate, which might be consistent with the presence of silicate features in the mid-IR spectrum (Evans et al. in preparation).

The lifespan of the dust emission in V745 Sco is short with the bump disappearing within a few days. Grain destruction may be by sputtering by high energy particles that diffuse across the shock fronts into the neutral zone or by the soft X-ray flux as proposed by Evans et al. (2017) for V339 Del and Gehrz et al. (2018) for V5668 Sgr.

2.3. *Site of the CO and dust*

Between days 8.5 and 11 when CO and dust were detected, the ejecta were extremely hot (a few times 10^7 K or more) because of shock heating (Banerjee et al. 2014; Orio et al. 2015; Drake et al. 2016). Collisional ionization is hence expected to be dominant, forming highly ionized species. It is very unlikely for molecules (CO) or dust to exist in this environment. Evidence for the high-ionization conditions prevailing in the ejecta on day 8.7 can be seen from Figure 3 wherein emission in several coronal lines are shown. Many of these ions, giving rise to the associated coronal lines, need energies $\gtrsim$350 eV to form. In addition to the high kinetic temperature prevailing in the shocked gas, modeling of the supersoft x-ray emission shows that the black body (BB) temperature of the central ionizing source, after having peaked at $\sim$ 95 eV (1.1×10^6 K) on day 5.5 – 6.5, was between 7.5×10^5 K and 6×10^5 K on days 8 to 10 respectively (Page et al. 2015). Thus the temperature was very high and the radiation field was harsh, and in such an environment it appears unlikely that molecules could form or grains condense within the ejecta.

However, in the radiative shock-driven model of Derdzinski et al. (2017) there exists a region where molecules and dust could potentially form. These authors show that as a

shock is driven into the ejecta, molecule and dust formation can occur within the cool, dense shell created between the forward and reverse shocks (Derdzinski et al. 2017, their Figure 1). While the forward and reverse shocks have temperatures of 10^7 K and a few megaKelvins respectively, the intermediate clumpy shell is cool and dense enough due to radiative shock compression (particle density $\sim 10^{14}$ cm^{-3}) to allow CO formation and rapid dust nucleation. We thus propose the CO/dust seen in V745 Sco formed in this region. Based on this framework, Figure 4 shows a schematic of the V745 Sco geometry. This figure includes important revisions to the system spatial dimensions necessitated by the recent revision of the orbital period (Schaefer 2022b) which differs significantly from earlier estimates.

Although (Schaefer 2009) had proposed the orbital period of V745 Sco was 510 $\pm$ 20 days , this was shown to be incorrect by Mróz et al. (2014, 2015) based on long term OGLE data. As a result Schaefer (2022a,b) has re-estimated the orbital period using the SED method. Assuming masses of the WD (M1) and RG (M2) to be 1.39 and 1.11 $M_\odot$ respectively, Schaefer (2022a) finds the $T_{eff}^{\rm RG}$ and radius $R_{\rm RG}$ of the secondary to be 2020 $\pm$ 60 K, and 370 $\pm$ 50 $R_\odot$ respectively and the orbital period to be 2440 $\pm$ 500 days. As the estimated $T_{eff}^{\rm RG}$ appeared to be on the lower side for a M6 III secondary, we have independently redone the analysis.

We constructed a SED using V, I magnitudes from OGLE (Mróz et al. 2015) as listed in SIMBAD, JHK magnitudes from 2MASS (Skrutskie et al. 2006), and WISE (Wright et al. 2010) W1, W2 magnitudes (E_{B-V}= 1.0 was used for dereddening). The WISE W3 and W4 magnitudes were excluded from the SED fit as they are heavily affected by dust in the V745 Sco system as shown by Spitzer spectra (Evans et al. in preparation). The SED analysis suggests $T_{eff}^{\rm RG}$ = 2350 $\pm$ 50 K with the corresponding radius of the donor being 290 $\pm$ 44 $R_\odot$ (assuming d = 8 $\pm$ 1 kpc). Assuming the star fills its Roche lobe, the orbital period is $\sim$ 1700 days, and orbital separation is $\sim$ 810 $R_\odot$. M1 and M2 are taken from Schaefer (2022a). We adopt these parameters in our analysis. These estimates of the orbital period and separation are marginally smaller (20% to 30%) than the Schaefer (2022a,b) estimates.

The spatial dimensions estimated above are used to prepare Figure 4 which is more or less to scale. Our primary focus is to locate the position of the clumpy CO and dust emitting zone with respect to the RG (i.e., did the CO form before or after the blast wave encountered the RG?). Figure 3 of Banerjee et al. (2014) shows the decline of the FWHM of the Paβ line with time. Taking the expansion velocity of the shock V(exp) as equal to half the FWHM, we find from the data of Banerjee et al. (2014) that V(exp) can be well represented by the polynomial V(exp) = v_0 + at + bt^2 + ct^3, with "t" being the time (in days) after outburst and with v_0 = 2689 km s^{-1}, a = -229, b = 5.45 and c = 0.075, respectively. Using the above polynomial, it is found the shock reaches the RG's WD-facing surface within 2 to 2.2 days. So it is obvious that the CO and dust, which formed between 8 to 10 days, did not form in the intervening gap between the WD and RG. In fact, at 8.7 d when the CO is detected, the CO emission zone was located $\sim$ 2000 $R_\odot$ away from the WD. That is, the shock had reached and engulfed the RG, refracted around it and was located at a distance of $\sim$ 2000 $R_\odot$ (9.3 au) from the WD when the dust/CO were detected.

It is moot to ask whether or not there is anything specific about the physical conditions (gas density, gas temperature, etc.) at this site/position that is specially favorable for dust/CO formation. However, it is essential to have newer 3D simulations that use the revised values for the orbital separation and radius of the donor instead of the old (but incorrect) values used by Orlando et al. (2017) which were: secondary star radius = 126 $R_\odot$; binary separation a = 1.7 au = 364 $R_\odot$. It would be of particular interest to see what the revised 3D simulations show and whether they can reproduce a clumpy, cool zone in between the forward shock (FS) and the reverse shock (RS) as predicted by (Derdzinski et al. 2017).

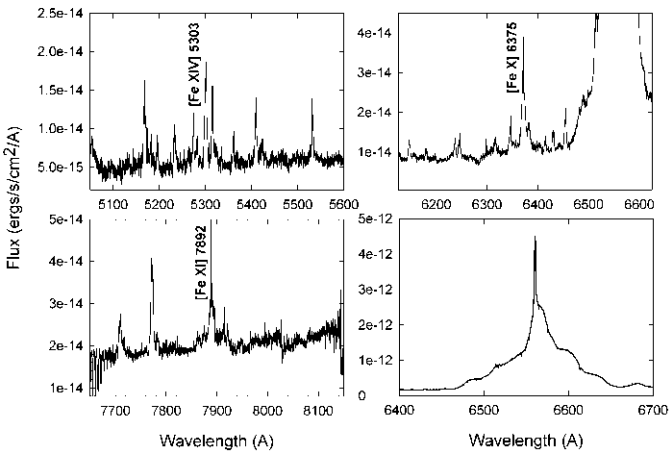

Figure 3. High resolution spectra (R = 120000) of V745 Sco obtained on the Cerro Tololo 1.3-m (+CHIRON) on 2014 Feb 16 ($\sim$ +10 d past outburst) showing coronal lines from highly ionized species. The Hα profile in the lower right panel is from 2014 Feb 09 ($\sim$ 3 days after the outburst) and shows structures which are discussed in the text.

3. DISCUSSION

This study presents a rare example of a nova in which dust and CO formation are likely triggered by shocks

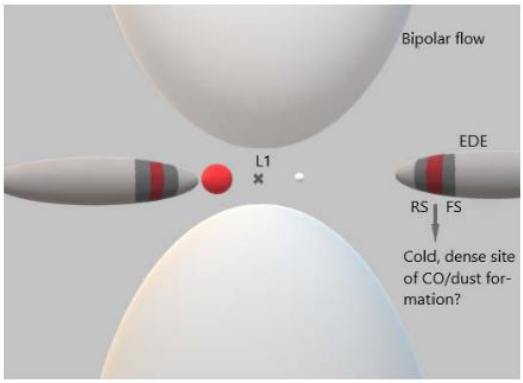

Figure 4. Schematic of the V745 Sco system with the equatorial density enhancement (EDE) that collimates the ejecta into a bipolar flow. The forward and reverse shocks (FS, RS) are shown with a cold clumpy shell in between that is proposed to be the site of the CO and dust formation. The positions and sizes of the WD, RG and shock region are roughly to the following scale (section 2.3) viz. $R_{RG} = 290\ R_\odot$, $R_{WD} = 65\ R_\odot$ (at outburst, Orlando et al. 2017), WD to RG separation = 810 $R_\odot$, inner Lagrangian point (L1) $\sim 450\ R_\odot$ from the WD. The distance of the FS from the WD is shown at 1070 $R_\odot$ assuming a representative value of the shock velocity, $v_s = 1000$ km s^{-1}. The actual distance lies at 2000 $R_\odot$, almost twice that shown. The shape of the EDE, as shown here, is only schematic.

(another example of a shock-induced dust forming nova is V2891 Cyg, Kumar et al. 2022) This study is also the first to record dust and CO formation in a RN. With typical recurrence timescales of a few tens of years and assuming a high mass accretion rate of $10^{-8}\ M_\odot$ yr^{-1}, not much more than $10^{-7}\ M_\odot$ can be accreted and subsequently ejected in a RN nova eruption. The ejecta are hence unlikely to be dense enough to be conducive to grain nucleation or molecule formation. It is however difficult to understand why similar systems (RS Oph, V407 Cyg, V3890 Sgr) failed to form CO and dust. All three objects have high cadence JHK spectra from the start of their respective outbursts; the first two on an almost daily basis (Das et al. 2006; Banerjee et al. 2009; Evans et al. 2022).

Among other plausible explanations, the blue-shifted CO emission seen in V745 Sco could be a consequence of the equatorial density enhancement (EDE) being viewed edge-on thereby hiding the receding red component from view. This needs to be verified through morpho-kinematic modeling (e.g., SHAPE, Steffen & Koning 2011) of high-resolution line profiles, for example the Hα profile in Figure 3. The shoulders in the Hα profile at $\sim$ 6480 and 6640 Å profile indicative a collimated polar flow and therefore give observational support for an EDE.

This study's robust evidence for a cool compressed zone between the forward shock (FS) and reverse shock (RS) suggests that the magnetic field lines from the RG should get compressed in this region due to the compression of matter (assuming the lines of force are frozen in; Tatischeff & Hernanz 2007). Future exploration is necessary to determine if this site is a region of particle acceleration (along the lines proposed for RS Oph in Tatischeff & Hernanz (2007, 2023)), thereby contributing to the generation of γ-rays.

4. SUMMARY

We have reanalyzed spectra and infrared light curve data of the recurrent nova V745 Sco shortly after its 2014 outburst. Carbon monoxide (CO) and dust in the ejecta of recurrent nova V745 Sco are reported. This is a rare instance of what appears to be shock-induced dust formation in a nova. The mass and temperature of the CO and dust are estimated to be $T_{CO} = 2250 \pm 250$ K, $M_{CO} = (1-5) \times 10^{-8}\ M_\odot$ and $T_{dust} = 1000 \pm 50$ K , $M_{dust} \sim 10^{-8}$ – $10^{-9}\ M_\odot$, respectively. Lastly, the site of the CO/dust emission, when it was first detected, is estimated to lie at $\sim 2000\ R_\odot$ (9.3 au) from the white dwarf. In comparison, the binary separation is 810 $R_\odot$.

ACKNOWLEDGMENTS

The authors wish to thank the referee for their insightful comments and detailed suggestions that improved the manuscript. This publication makes use of data products from the Wide-field Infrared Survey Explorer (https://doi:10.26131/IRSA142), which is a joint project of the University of California, Los Angeles, and the Jet Propulsion Laboratory/California Institute of Technology, funded by the National Aeronautics and Space Administration. This publication makes use of data products from the Two Micron All Sky Survey (https://doi:10.26131/IRSA2), which is a joint project of the University of Massachusetts and the Infrared Processing and Analysis Center/California Institute of Technology, funded by the National Aeronautics and Space Administration and the National Science Foundation. This publication, in part, is based on observations at Cerro Tololo Inter-American Observatory at NSF's NOIRLab, which is managed by the Association of Universities for Research in Astronomy (AURA) under a cooperative agreement with the National Science Foundation.

Facilities: 2MASS, OGLE, WISE, CTIO:1.3m, ANDICAM, CHIRON

Software: Astropy (Astropy Collaboration et al. 2018)

REFERENCES

Anupama, G. C., & Mikołajewska, J. 1999, A&A, 344, 177, doi: 10.48550/arXiv.astro-ph/9812432

Astropy Collaboration, Price-Whelan, A. M., Sipőcz, B. M., et al. 2018, AJ, 156, 123, doi: 10.3847/1538-3881/aabc4f

Banerjee, D. P. K., Das, R. K., & Ashok, N. M. 2009, MNRAS, 399, 357, doi: 10.1111/j.1365-2966.2009.15279.x

Banerjee, D. P. K., Joshi, V., Venkataraman, V., et al. 2014, ApJL, 785, L11, doi: 10.1088/2041-8205/785/1/L11

Banerjee, D. P. K., Srivastava, M. K., Ashok, N. M., & Venkataraman, V. 2016, MNRAS, 455, L109, doi: 10.1093/mnrasl/slv163

Cheung, C. C., Jean, P., & Shore, S. N. 2014, The Astronomer's Telegram, 5879, 1

Das, R., Banerjee, D. P. K., & Ashok, N. M. 2006, ApJL, 653, L141, doi: 10.1086/510674

Das, R. K., Banerjee, D. P. K., & Ashok, N. M. 2009, MNRAS, 398, 375, doi: 10.1111/j.1365-2966.2009.15141.x

Derdzinski, A. M., Metzger, B. D., & Lazzati, D. 2017, MNRAS, 469, 1314, doi: 10.1093/mnras/stx829

Draine, B. T., & Lee, H. M. 1984, ApJ, 285, 89, doi: 10.1086/162480

Drake, J. J., Delgado, L., Laming, J. M., et al. 2016, ApJ, 825, 95, doi: 10.3847/0004-637X/825/2/95

Duerbeck, H. W. 1989, The Messenger, 58, 34

Evans, A., Geballe, T. R., Rawlings, J. M. C., & Scott, A. D. 1996, MNRAS, 282, 1049, doi: 10.1093/mnras/282.3.1049

Evans, A., Geballe, T. R., Woodward, C. E., et al. 2022, MNRAS, 517, 6077, doi: 10.1093/mnras/stac2363

Evans, A., & Gehrz, R. D. 2022, arXiv e-prints, arXiv:2211.12410, doi: 10.48550/arXiv.2211.12410

Evans, A., Woodward, C. E., Helton, L. A., et al. 2007, ApJL, 671, L157, doi: 10.1086/524944

Evans, A., Banerjee, D. P. K., Gehrz, R. D., et al. 2017, MNRAS, 466, 4221, doi: 10.1093/mnras/stw3334

Gehrz, R. D., Truran, J. W., Williams, R. E., & Starrfield, S. 1998, PASP, 110, 3, doi: 10.1086/316107

Gehrz, R. D., Evans, A., Woodward, C. E., et al. 2018, ApJ, 858, 78, doi: 10.3847/1538-4357/aaba81

Harrison, T. E., Johnson, J. J., & Spyromilio, J. 1993, AJ, 105, 320, doi: 10.1086/116429

Joshi, V., Banerjee, D. P. K., & Srivastava, M. 2017, ApJL, 851, L30, doi: 10.3847/2041-8213/aa9d86

Kantharia, N. G., Dutta, P., Roy, N., et al. 2015, in Astronomical Society of India Conference Series, Vol. 12, Astronomical Society of India Conference Series, 107–108, doi: 10.48550/arXiv.1510.01120

Kumar, V., Srivastava, M. K., Banerjee, D. P. K., et al. 2022, MNRAS, 510, 4265, doi: 10.1093/mnras/stab3772

Mróz, P., Poleski, R., Udalski, A., et al. 2014, MNRAS, 443, 784, doi: 10.1093/mnras/stu1181

Mróz, P., Udalski, A., Poleski, R., et al. 2015, ApJS, 219, 26, doi: 10.1088/0067-0049/219/2/26

Orio, M., Rana, V., Page, K. L., Sokoloski, J., & Harrison, F. 2015, MNRAS, 448, L35, doi: 10.1093/mnrasl/slu195

Orlando, S., Drake, J. J., & Miceli, M. 2017, MNRAS, 464, 5003, doi: 10.1093/mnras/stw2718

Page, K. L., Osborne, J. P., Kuin, N. P. M., et al. 2015, MNRAS, 454, 3108, doi: 10.1093/mnras/stv2144

Pontefract, M., & Rawlings, J. M. C. 2004, MNRAS, 347, 1294, doi: 10.1111/j.1365-2966.2004.07330.x

Rudy, R., Mauerhan, J., Crawford, K., Russell, R., & Wiktorowicz, S. 2018, The Astronomer's Telegram, 11565, 1

Russell, R. W., Sitko, M. L., Rudy, R. J., et al. 2020, The Astronomer's Telegram, 13967, 1

Schaefer, B. E. 2009, ApJ, 697, 721, doi: 10.1088/0004-637X/697/1/721

—. 2022a, MNRAS, 517, 3640, doi: 10.1093/mnras/stac2089

—. 2022b, MNRAS, 517, 6150, doi: 10.1093/mnras/stac2900

Sekiguchi, K., Whitelock, P. A., Feast, M. W., et al. 1990, MNRAS, 246, 78

Simcoe, R. A., Burgasser, A. J., Bernstein, R. A., et al. 2008, in Society of Photo-Optical Instrumentation Engineers (SPIE) Conference Series, Vol. 7014, Ground-based and Airborne Instrumentation for Astronomy II, ed. I. S. McLean & M. M. Casali, 70140U, doi: 10.1117/12.790414

Skrutskie, M. F., Cutri, R. M., Stiening, R., et al. 2006, AJ, 131, 1163, doi: 10.1086/498708

Speck, A. K., Barlow, M. J., Sylvester, R. J., & Hofmeister, A. M. 2000, A&AS, 146, 437, doi: 10.1051/aas:2000274

Steffen, W., & Koning, N. 2011, in Asymmetric Planetary Nebulae 5 Conference, P59

Tatischeff, V., & Hernanz, M. 2007, ApJL, 663, L101, doi: 10.1086/520049

—. 2023, arXiv e-prints, arXiv:2302.01276, doi: 10.48550/arXiv.2302.01276

Walter, F. M., Battisti, A., Towers, S. E., Bond, H. E., & Stringfellow, G. S. 2012, PASP, 124, 1057, doi: 10.1086/668404

Williams, R. E., Hamuy, M., Phillips, M. M., et al. 1991, ApJ, 376, 721, doi: 10.1086/170319

Woodward, C. E., Banerjee, D. P. K., & Evans, A. 2020, The Astronomer's Telegram, 14034, 1

Wright, E. L., Eisenhardt, P. R. M., Mainzer, A. K., et al. 2010, AJ, 140, 1868, doi: 10.1088/0004-6256/140/6/1868

Zubko, V. G., Mennella, V., Colangeli, L., & Bussoletti, E. 1996, MNRAS, 282, 1321, doi: 10.1093/mnras/282.4.1321